LAWRENCE
LIVERMORE
NATIONAL
LABORATORY

UCRL-JRNL-206068

# Self-Organization Observed in Numerical Simulations of a Hard-Core Diffuse Z Pinch

V. Makhin, R. E. Siemon, B. S. Bauer, A. Esaulov, I. R. Lindemuth, D. D. Ryutov, P. T. Sheehey, V. I. Sotnikov

August 16, 2004

Physics of Plasmas

# Self-organization observed in numerical simulations of a hard-core diffuse z pinch

V. Makhin, R.E. Siemon, B.S. Bauer, A. Esaulov,

I.R. Lindemuth, D.D. Ryutov[1)], P.T. Sheehey[2)], V.I. Sotnikov

## I. Introduction

The idea of Magnetized Target Fusion (MTF) has attracted increased interest in recent years, because it might overcome the problem of high costs associated with conventional magnetic or inertial fusion approaches.[1] If MTF is interpreted in the general sense to mean any pulsed system that works in a high-energy-density regime and uses a magnetic field to improve energy confinement at peak compression, then it is clear from recent publications that there are a large variety of possible driver and plasma target combinations for MTF.[2,3,4,5,6] For the target, a stable high-$\beta$ plasma equilibrium is desired, with energy confinement as good as Bohm or better.[7] The focus of this paper is the stability of one MTF possibility — the hard-core stabilized z pinch. Although equilibrium and stability of a z pinch has been discussed in many papers and books, there is renewed interest in the subtleties of z-pinch stability for application to MTF as well as other topics. Pulsed power has been used in recent years to generate unprecedented radiation pulses from wire-array z pinches,[8] shear flow has been demonstrated to provide

[1] Also at Lawrence Livermore National Laboratory, Livermore, CA 94550
[2] Also at Los Alamos National Laboratory, Los Alamos, NM 87545

an interesting stabilizing effect,[9] and the diffuse z pinch has many features in common with dipole confinement also being studied for its potential to fusion.[10]

The hard-core stabilized target of interest, shown in Fig. 1, differs from an ordinary diffuse z pinch because of the current-carrying central conductor, or hard core, that is helpful for forming a stable equilibrium in the absence of shear flow. In this geometry, the plasma carries the return current of the central conductor, whereas in the more traditional z-pinch, the plasma carries the central current and the return current is carried by outer conductors. The direction of current in the plasma is indicated schematically in Fig. 1 as opposite to the direction of current in the hard core, which is the situation during plasma formation. Later in time, when equilibrium is obtained, current in the plasma flows in different directions at different radial locations as discussed below. The plasma is bounded in the axial direction by room-temperature electrodes not shown. In a stable plasma, energy confinement is presumably dominated by a combination of cross-field thermal conduction in the presence of convective cells, and a heat flux carried by the current moving through the plasma. This paper focuses on how plasma self-organizes itself into a stable equilibrium with a pressure profile like that shown in Fig. 2. We plan to address issues of energy confinement in future work.

The MAGO experiments, studied at the VNIIEF laboratory in Russia, appear to create this type of plasma configuration using a unique dual chamber method to shock heat the plasma.[11] In MAGO the plasma may carry either the applied current or the return current,

or both, depending upon the plasma dynamics, because of the unique insulator location and breakdown across a nozzle.

A coaxial geometry would adapt readily to various high-voltage high-current implosion drivers such as Shiva Star at the Air Force Research Laboratory, Atlas at the Nevada Test Site, or explosive pulsed power systems such as those developed in Russia at the VNIIEF laboratory. Also, a new experiment at the University of Nevada, Reno (UNR), is being prepared to study wall-plasma interactions for this type of configuration. According to numerical simulations of plasma heating and formation, existing hardware with minor modifications could be used for the UNR experiment.[12]

In section II we review some well known properties of equilibrium and stability in a diffuse z pinch, and introduce the nomenclature that will be used for discussion of simulation results. Section III presents the an example of self-organization obtained using two-dimensional simulations of the plasma formation process. Section IV examines some interesting details of how interchange motion driven by instability converts an unstable pressure profile into one that is stable starting with an idealized initial condition that is easier to analyze than the relatively complex process of plasma formation. Section V discusses and summarizes the results.

**II. Review of equilibrium and stability for the stabilized hard-core z pinch**

Assuming we have a purely azimuthal magnetic field with current flowing only in the r and z directions, the only equilibrium solution possible has pressure contours and current

contours that are nested cylinders aligned with the z axis. Current and pressure depend only upon the radius, and there is no radial current in an equilibrium. Otherwise, contours of pressure and current could not coincide, as they must for ***jxB*** to equal $\nabla p$. In two-dimensional numerical simulations to be discussed later in this paper, current flows in both the radial and axial directions, and the evolution of plasma towards an equilibrium of nested cylinders is observed during simulations. One implication for the diffuse z-pinch geometry is that a system of finite length must have pressure balanced in the axial direction by material walls (*eg*., electrodes). Thermal losses are mitigated however by the fact that the heat must flow across the magnetic field.

Pressure balance in equilibrium can be written as follows:

$$I(r)^2 = -\frac{8\pi^2}{\mu_0}\int r^2 \frac{dp}{dr} dr \ , \qquad (1)$$

where the integrated current inside the radius $r$, $I(r) = 2\pi rB/\mu_0$, is often a more convenient variable than $B(r)$ or $j_z = \frac{1}{r}\frac{\partial}{\partial r}\left(rB(r)\right)$. Using Eq. 1, the thermal energy per unit length $U$ between radius $a$ and $b$ can be written:

$$U = \frac{3\mu_0}{16\pi}\delta\left[(\beta+1)I^2\right], \qquad (2)$$

where $\delta F(r) \equiv F(b) - F(a)$.The quantity $\beta(r)$ is the ratio of $p(r)$ to magnetic pressure evaluated at the same radius. The right hand side of Eq. 2 can be thought of as diamagnetism in a z pinch, with thermal energy approximately proportional to $I\delta I$. Eq. 2 is one way to write the Bennet relationship for uniform temperature pinches, in which $NkT$ is proportional to $I^2$, where N is the number of particles per unit length.

As shown early on by Kadomtsev,[13] such an equilibrium will be stable to $m = 0$ interchanges provided that the gradient in pressure $p(r)$ is small enough anywhere pressure decreases as radius increases. The Kadomtsev criterion can be written $Q < 1$ where (for $\gamma = 5/3$):

$$Q = \frac{-20}{(6+5\beta)} \frac{r}{p} \frac{dp}{dr} \tag{3}$$

For stability to higher $m$ modes, Kadomtsev derives the additional requirement:

$$-\frac{r}{p}\frac{dp}{dr} < \frac{m^2}{\beta} \tag{4}$$

If the pressure profile is marginally stable to $m$=0 with Q=1, Eqs. 3 and 4 show that the modes with $m = 1$ or higher are stable if the maximum $\beta$ is less than 2/5. From the perspective of MTF, it is interesting to note that stability depends only on the gradient of pressure, so if pressure is supported by a conducting boundary it should be possible to have stability at any $\beta$ provided the logarithmic gradient is sufficiently small. The numerical studies in this paper are motivated by experimental design. To avoid $m = 1$ modes, the effects of which can not be investigated numerically in a two-dimensional code, we have chosen parameters that produce $\beta$ less than 2/5, but this may be overly conservative.

One example of an equilibrium stable to all modes is shown in Fig. 2. In the radial region beyond the peak pressure, Fig. 2 shows the shape of the Q=1 marginally stable profile. The $\beta$ at peak pressure is 2/5. Inside the point of peak pressure, the shape of the profile is

arbitrary provided the pressure increases monotonically with radius, because then Q is negative and clearly less than 1. In the limit where the pressure changes as a step function at the point of maximum pressure, Eq. 2 shows that $(\beta+1)I^2$ is continuous across the step, which relates the change of current to the change in β. The marginally stable pressure profile, derived by integrating Eq. 3 with Q = 1, can only be written in parametric form:[14]

$$\frac{p}{p_0} = \frac{\beta^{5/2}}{(0.8+\beta)^{5/2}} \tag{5}$$

$$\frac{r}{a} = \frac{(0.8+\beta)^{1/4}}{\beta^{3/4}} \tag{6}$$

$$\frac{I}{I_0} = \frac{1}{0.8+\beta} \tag{7}$$

The current $I$ follows from Eqs. (5) and (6) because $B = \sqrt{2\mu_0 p/\beta}$ , and the parameter $I_0$ can be expressed in terms of $p_0$ and $a$. The parameters $p_0$ and $a$ are set by choosing the maximum pressure and $\beta$ value at a particular radius. The pressure profile can be computed all the way to the axis in the absence of a hard core (dotted line in Fig. 2), but in that case $\beta$ goes to infinity at the axis, and the m=1 or higher modes are unstable with any finite pressure gradient. Thus a hard-core conductor allows stability to all MHD modes with a static equilibrium (no velocity) supported by arbitrarily small pressure at the wall in the radial direction. Non-static possibilities are shear flow stabilization,[15] or possibly dynamic stabilization.[16]

**III. Self-organization in simulations of experimental plasma formation.**

In designing the UNR experiment to study wall-plasma interactions in this geometry, it was initially hoped that control of formation parameters (voltage, fill pressure, bias current, etc.) would make it possible to generate the type of stable profile shown in Fig. 2 and discussed in Sec. II. Such profiles have been characterized in textbooks as theoretically possible but difficult to achieve in experiment.[17] As reported earlier, it was not possible with one-dimensional simulations to generate stable profiles except for very limited conditions, and then only during a brief interval of time.[12] The subsequent, more realistic two-dimensional simulations reported in this paper show in detail how interchange motions can self-organize the plasma into a stable profile.

To simulate the experimental formation process, the geometry and current wave form are chosen to be compatible with existing hardware.[12] The hard core is assumed to be 32-cm long and to have a 2-cm radius with a thin insulating cover. The outer return conductor is assumed to be metal with an inner radius of 10 cm. For the plasma, the initial conditions are taken to be a uniform annulus of fully ionized 1-eV deuterium between 2 and 3 cm with density $8 \times 10^{-4}$ kg/m$^3$ (3.5 torr). This distribution of initial plasma is an idealized version of what could be created with puff valves in an experiment. The temperature of 1 eV is not a critical parameter, and is chosen to give a reasonably small resistivity at the beginning of the calculation so that a diamagnetic current sheet forms in the plasma as current in the hard core increases. Experience with simulation of pulsed experiments has shown that the details of ionization physics can usually be ignored during a fast-rising current ramp because ionization energy requirements are small compared with ohmic

heating, and shock heating processes under high-voltage conditions. A peak-to-peak 0.1% random perturbation of density is included in the initial conditions to seed Rayleigh-Taylor like modes during the dynamic phase as described below. For the simulation, the inner radial boundary at r=2 cm is assumed to be an insulator on which current is specified to rise with a prescribed function of time. The outer radial boundary at r=10 cm is taken as a zero temperature electrical conductor, which absorbs heat with no change in temperature. The same type of electrical conductor is assumed at the top boundary (half length z = 16 cm), which represents the end electrodes in an experiment. The other boundary of calculation is assumed to be a reflecting boundary or plane of symmetry, at the axial midplane (z=0).

The current wave form used in this simulation is the same as expected in experiments with the UNR Zebra power supply. An initial bias current of 300 kA is assumed to exist at t = 0, which would come from a slow-rising capacitor bank in the experiment. Maximum $\beta$ in the final plasma equilibrium decreases as bias current increases. The bias current of 300 kA was chosen because maximum $\beta$ in that case is about 0.4, which satisfies the $m$=1 stability constraint as discussed in Sec. II. High voltage (2MV) is applied at t=0, and current increases by about 1 MA in 100 ns. After that the current becomes constant in time with an amplitude of about 1.2 MA because of crowbar action in the experiment when current flashes over on the final insulator of the Zebra device (a different component than the insulator on the hard core). The gas is ionized, accelerated outwards, and shock heated by a current sheet that forms during the fast current rise. The

time-varying impedance represented by the moving current sheet has a negligible affect on the output waveform of the generator.

A two-temperature single-fluid magnetohydrodynamic (MHD) model is used for simulations, with Braginskii coefficients of thermal conduction and electrical resistivity.[12] The assumed Ohm s law is $\boldsymbol{E}+\mathbf{v}\mathrm{x}\boldsymbol{B} = \eta\boldsymbol{j}$, which relates electric field **E**, fluid velocity **v**, magnetic field **B**, current **j**, and resistivity η. A vonNeumann-Richtmyer numerical viscosity is introduced to dissipate energy from shock waves in a manner that conserves mass, momentum, and energy. As is well known, such a viscosity is required to obtain accurate solutions to the MHD equations unless shock-tracking methods are used, i.e., use of the numerical viscosity makes the calculations more accurate than they would be otherwise. Most calculations were done with an array of 100x100 zones, using progressively finer-scale resolution near low-temperature boundaries to improve accuracy. It was found that a factor of 2 reduction in resolution changes results by less than 10%. Higher resolution has yet to be implemented, and will entail larger data files and even greater computational time. Typical simulations with 100x100 resolution require about 4 hours on a Pentium 4 processor and generate 500 MB of data.

The time history of kinetic energy and thermal energy is shown in Fig. 3. The first peak of kinetic energy occurs as the inverse pinch drives the plasma outwards, and then kinetic energy goes to a minimum when the plasma compresses bias flux up against the outer conductor and stagnates at about 280 ns. Compressional Alfven waves oscillate back and forth radially while directed energy is converted into thermal energy. Between 1 and 2

μs, most of the shock heating (i.e., the kinetic energy dissipated by the numerical viscosity) has subsided and plasma temperature is about 420 eV.

Figure 4 shows contours of pressure (color) and current (lines) at four moments in time. At the first point of stagnation (t = 280 ns) the plasma shows little sign of Rayleigh-Taylor-like (RT) modes even though outward and inward acceleration has occurred. Near the next point of stagnation (t = 400 ns) RT modes are starting to grow from the initial random density perturbation. As discussed in Reference 11, the growth rate for RT modes agrees qualitatively with the expected $\gamma \sim (ak)^{1/2}$, where a is the plasma acceleration and k is the axial wave length. However, as noted elsewhere,[18] quantitative comparison is difficult given that acceleration is not uniform throughout the plasma, and has a complicated time history. In addition, curvature-driven m=0 modes of the type discussed by Kadomtsev can occur as the plasma seeks equilibrium. At t = 700 ns, two oscillations have taken place, and the Richtmeyer-Meshkov (RM) process has generated pronounced spikes on the inner boundary of the plasma. The association with RM is based on the qualitative observation that the density shows very rapid development of spikes when a shock propagating from the outer wall passes over the plasma density gradient. By t = 1.65 us, the plasma is beginning to settle into an equilibrium, although the pressure contours have a strong granularity that remains from the RT and RM modes.

An equilibrium with pressure and current contours uniform in z is not apparent in the contour plots of Fig. 4. Because of the RT-like and curvature-driven *m*=0 instabilities the plasma is generally in a state of fluctuation away from equilibrium even after radial

dynamics have dissipated. A perturbation analysis of equilibrium shows that first order perturbations in plasma or magnetic pressure give rise to second order corrections to equilibrium balance between $\boldsymbol{jxB}$ and $\boldsymbol{\nabla} p$. Thus, provided the fluctuations are reasonably small, one expects equilibrium to exist in an average sense even for a granular structure like that shown at 1.65 μs in Fig. 4.

To examine equilibrium and stability properties for simulation results, we use z-averaged quantities for variables such as pressure. For example, the symbol $p(r)$ is defined within the computational domain of length Z to be:

$$p(r) \equiv \frac{1}{Z}\int_0^Z p(r,z)dz \tag{8}$$

We find that the discussion of Sec. II applies approximately to the z averaged quantities with increasing accuracy as temporal fluctuations from the formation dynamics fade away. To investigate the approach to equilibrium during the dynamic formation phase, we compute a quantity Δ defined as the difference between thermal energy per unit length and diamagnetism as introduced in Eq. 2:

$$\Delta \equiv U - \frac{3\pi}{16}\delta[(1+\beta)I^2] \tag{9}$$

We take the limits of integration to include the entire computational domain, so U is the total thermal energy per unit length in the computation, and δ is evaluated at the inner and outer radius. We know from Eq. 2 that in a static equilibrium Δ is zero. When the

$\rho Dv/Dt$ term is considered, the equation of motion in one dimension can be used to show:

$$\Delta = \frac{3}{2} KE/Z + \frac{3\pi}{2}\delta[r^2 \rho v^2] + \frac{3\pi}{2}\frac{\partial}{\partial t}\int_a^b \rho v r^2 dr \qquad (10)$$

Thus Δ is a measure of departure from equilibrium at least for one-dimensional behavior. As velocity and oscillatory motion approach zero, Eq. 10 shows that delta should approach zero. Despite the complicated structure of 2D equilibrium as seen in Fig. 3, the value of Δ computed with z-averaged values from the simulation approaches zero as equilibrium is established, as shown in Fig. 5. The main contribution to the oscillations seen in Fig. 5 comes from the inertial term (last term in Eq. 10).

Next we show the approach to stability using z-averaged pressure profiles. During the formation phase with radial oscillations, the profiles obtained in simulations always show regions where Q > 1. However, as time progresses, the radial oscillations subside, RT modes fade away, and the pressure profile settles into a Kadomtsev-stable profile. This is shown in Fig. 6 where z-averaged pressure profiles are displayed at two moments of time. A marginally stable Kadomstsev profile is also shown with a heavy line for comparison. The profile shown at 8 microseconds is very close to the marginal state outside r = 7 cm (ie., Q ~ 1), and the inner region has Q < 1. A computer-generated movie of the sequence of these pressure profiles gives the impression that the plasma is being gradually forced by oscillations into a stable state that appears first at large radius and then at smaller and smaller radius.

This qualitative evolution to stability has been observed under a variety of initial conditions pertinent to the experiment being planned. Sometimes, the pressure profile obtained has more than one point of maximum pressure and does not much resemble the profile in Fig. 2, but the value of Q appears to evolve in any case towards a value less than unity at all radial locations except near cold boundaries. Presumably, although this has not been checked in detail, the few-mm-thick cold boundary is evolving more slowly because the thermal speed gets so small.

**IV. Self-organization in simulations starting with idealized unstable equilibrium**

The process of self-organization can be studied more readily if the initial conditions are a well defined static equilibrium instead of dynamic formation like that in an experiment, such as illustrated in the previous section. A static equilibrium was selected with Q = 1.1, which makes the pressure gradient uniformly larger than the marginal profile required for stability. The profile looks very similar to Fig. 2 (solid line), but with a slightly larger gradient that drops from the same peak value to a pressure at the wall about 2/3 of the value in Fig. 2. All boundaries for these simulations are reflecting boundaries like the boundary at z=0 in the previous simulation. This prevents thermal conduction from transferring energy out of the computational region during the development of instability. The maximum pressure is taken as $5 \times 10^7$ Pa at r = 3 cm, and maximum $\beta$ is 0.40. The corresponding current on the hard core is 1 MA. The initial conditions are completed by setting temperature as uniform equal to 300 eV, and by adding a 0.2% peak-to-peak sinusoidal density perturbation with an axial wavelength of 4 cm.

It might seem that the final plasma state following interchange would become exactly a Q = 1 profile based on the expected tendency to evolve towards stability. That is not the case because the particular shape of a Q=1 profile has different values of flux and total energy (thermal plus magnetic) than the Q=1.1 profile. For the case at hand, the difference is small, because flux and total energy for a Q=1 profile with the same peak pressure (same hard-core current) differs from a Q=1.1 profile by only a few percent. Never-the-less, this reasoning shows that the plasma relaxes to something with Q less than or equal to unity everywhere, but not exactly Q=1.

Fig. 7 shows contour plots of mass density in color, and stream lines of velocity. The interchange mode evolves much like a Rayleigh-Taylor mode with bubbles and spikes at the expected locations. Unlike the formation process described in Sec. III, there is no accelerated frame of reference in this simulation giving rise to an effective gravity. The effective gravity comes from field line curvature with acceleration equal to $V_i^2/R$, where $V_i$ is the ion thermal speed, and R is the field line curvature.[19] The growth rate in the simulation can be determined by the exponential growth of kinetic energy at early times. A least squares fit gives $\gamma = 3.5 \pm .3 \times 10^7$ sec$^{-1}$ during the first microsecond of growth. The uncertainty arises mainly from numerical noise introduced by round-off errors in equilibrium at t = 0. A δW calculation has not been done for this profile to our knowledge, but the approximate expression[19] for $\gamma = 2\sqrt{a/s}$ , where *s* is the density gradient length and *a* is the effective acceleration, gives $\gamma \sim 1 \times 10^7$ sec$^{-1}$. The growth rate observed with other values of Q and perturbation wave length are listed in Table 1.

| $\lambda_z$ (Q=1.1) | $\gamma$ | Q ($\lambda_z$ = 4 cm) | $\gamma$ |
|---|---|---|---|
| 2 cm | $3.5 \times 10^6$ sec$^{-1}$ | 1.1 | $3.5 \times 10^6$ sec$^{-1}$ |
| 4 cm | $3.2 \times 10^6$ sec$^{-1}$ | 1.01 | $2.2 \times 10^6$ sec$^{-1}$ |
| 8 cm | $3.3 \times 10^6$ sec$^{-1}$ | 1.000001 | $2.1 \times 10^6$ sec$^{-1}$ |

Table 1. Growth rates of *m*=0 mode for various values of Q and perturbation wavelength in the axial direction.

The interchange nature of the mode with convective cells is apparent from the velocity stream lines. Where the perturbed density is maximum (z=0, 4, 8 cm), pressure is larger than ***jxB*** and plasma moves outward and develops nonlinearly into bubbles. At the anti nodes, the opposite occurs and the motion develops nonlinearly into spikes.

The unstable interchange motion that develops can be divided into two phases: a coherent phase that grows in a predictable way from the initial perturbation, followed by an incoherent or chaotic turbulent phase which has no discernable relationship with the initial conditions. In Fig. 7 the coherent phase is shown in the first three frames, and the

incoherent phase has begun in the fourth frame at 2.85 μs. During the coherent phase, kinetic energy of the interchange motion comes from thermal energy through adiabatic PdV work on the plasma. This is seen graphically in Fig. 8, where kinetic energy and thermal energy are plotted vs. time. In 2.6 μs kinetic energy grows to 85 J, while thermal energy drops by the same amount from an initial value of 12.2 kJ. The values of U and EM plotted in Fig. 8 are actually (U-12,200) and (EM-17,500) in order to see the changes in U and EM on the same scale as KE, PdV, and shock heating. The pdV work in the simulation, shown in the lower graph of Fig. 8, equals the kinetic energy during the coherent phase of instability growth. Then as the mode develops into a nonlinear phase, steep gradients develop and the vonNeumann-Richtmyer viscosity begins to dissipate energy through shock heating. The transition from coherent to incoherent motion occurs at about 2.8 μs, slightly later in time than the peak of kinetic energy where shock heating begins. When viewed as a movie the transition is quite abrupt and the onset of incoherent motion could be described as explosive. The PdV work equals the change in thermal energy, as shown in part (b) of Fig. 8.

During the interchange motion of instability, plasma moving inward is heated as it is compressed, and plasma moving outward is cooled as it expands. The z-averaged temperature, initially uniform with T = 300 eV, becomes considerably larger at small radius (500-1000 eV), and smaller at large radius, but during the coherent phase of motion, the average value is not very meaningful. This is illustrated in Fig. 9, which shows contours of temperature near the end of the coherent phase of motion. Fig. 10 shows the adiabatic nature of the motion, by examining the temperature along a line

where plasma is flowing inward and getting compressed. The temperature according to the simulation is compared with a prediction (shown as cross-hatched points) based on constant entropy ($p/\rho^{5/3}$). The motion of fluid elements from an earlier moment at the same axial location (t=1 μs when T ~ 320 eV) is deduced by assuming fluid elements conserve flux ($d\phi = B\, dr\, dz$) and mass ($dM=\rho\, 2\pi\, r\, dr\, dz$), which means the ratio $B/\rho r$ can be used to identify the moving fluid elements. In other words, locations in the plasma with the same value of $B/\rho r$ at different times, can be associated with the location of fluid elements, which heat according to constant $p/\rho^{5/3}$. After the coherent phase ends and the plasma enters a turbulent state, the z-averaged temperature profile is more meaningful in the sense of less variation along z, and quits evolving in time. The profile would be difficult if not impossible to predict because it depends upon the detailed non-linear evolution of the plasma motion. Simulations show that the final maximum z-averaged temperature profile can differ by as much as 300 eV, depending upon the level of density perturbation introduced and whether it is introduced as a sinusoid or a random perturbation.

**V. Conclusions.**

The evolution of an unstable plasma profile into a stable profile, which we term self-organization, appears to be a robust process. Although it was not termed self organization, the same effect has been noted in past simulations with the same code.[20] The result has been made easier to discern by the introduction of z-averaged profiles. A recent report of PIC simulations in the hard-core z-pinch configuration also shows self-

organization.[21] Figures 3 and 4 in Reference 21 show how pressure profiles in a low-β PIC simulation relax from unstable to stable.

The non-linear evolution of the interchange motion has been studied under controlled initial conditions that result in exponential growth of a mode with a prescribed axial wavelength. An interesting feature of such growth is an abrupt transition from coherent to incoherent motion, after which the z-averaged pressure, current, and temperature profiles become quasi stationary.

According to our understanding of MAGO experiments, the observed plasma behavior is consistent with the expectation of self-organization, but the diagnostics are not sufficiently detailed thus far to make a definite conclusion.[22] The results of this simulations reported in this paper add motivation to planned experiments on an inverse pinch at UNR.

This work was performed under the auspices of the U. S. Department of Energy by University of California, Lawrence Livermore National Laboratory under contract W-7405-Eng-48.

FIGURES and CAPTIONS

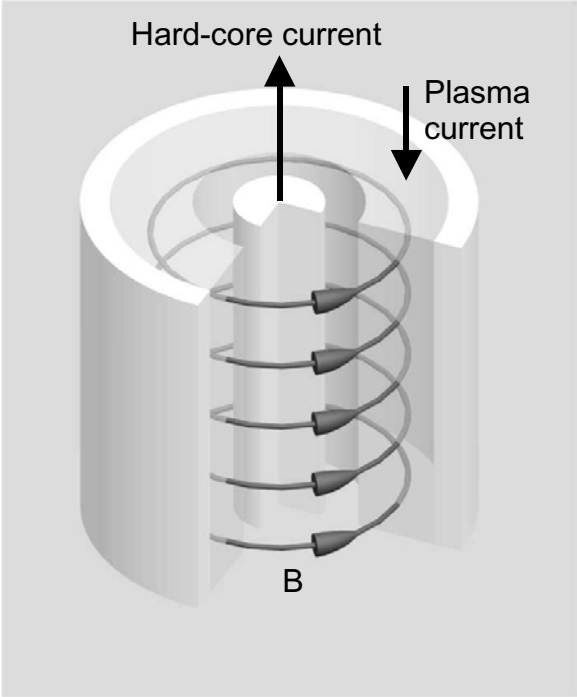


Fig. 1. Geometry of hard-core diffuse z pinch. Axial currents produce $B_\theta$ magnetic field.

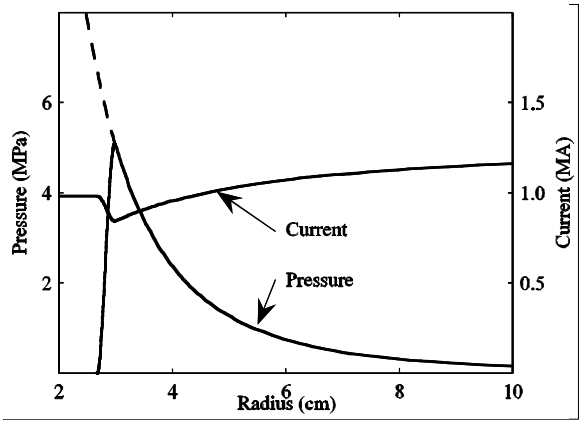


Fig. 2. An example of an MHD-stable current and pressure profile in a hard-core diffuse z pinch. The equilibrium current can be computed from the pressure using Eq. 1.

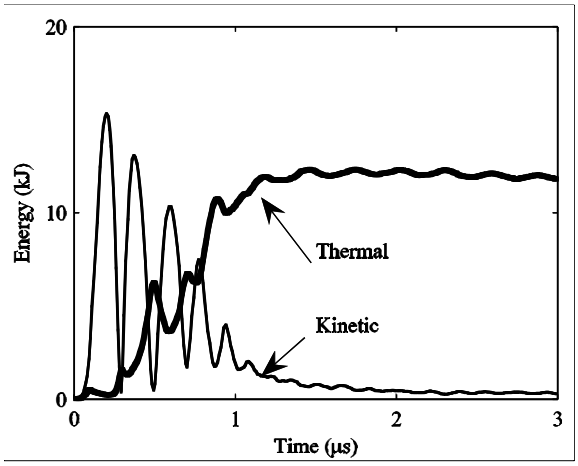

Fig. 3. Simulation results for thermal energy (heavy line) and kinetic energy (thin line) vs. time during plasma formation and heating in an inverse pinch.

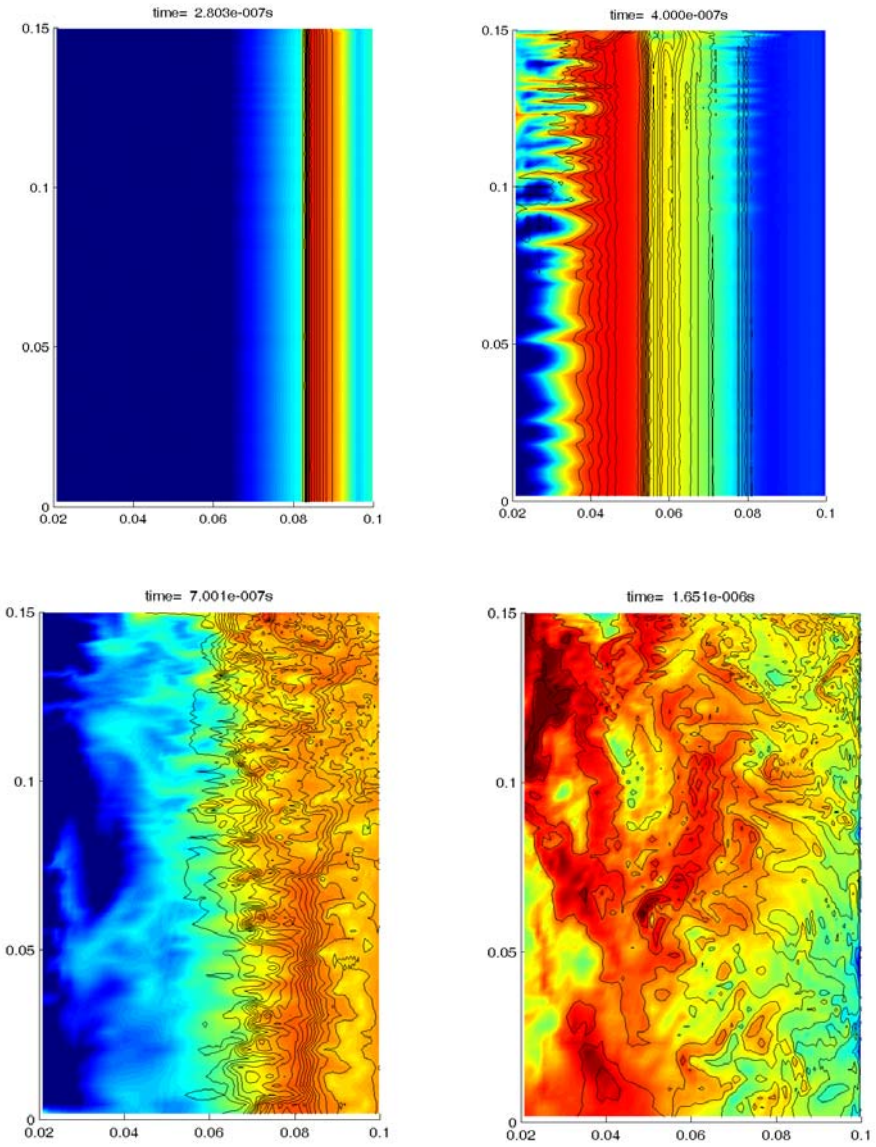


Fig. 4. Contour plots in r and z at indicated times showing transition from dynamic to equilibrium phase. Color is pressure contours and lines are total current contours.

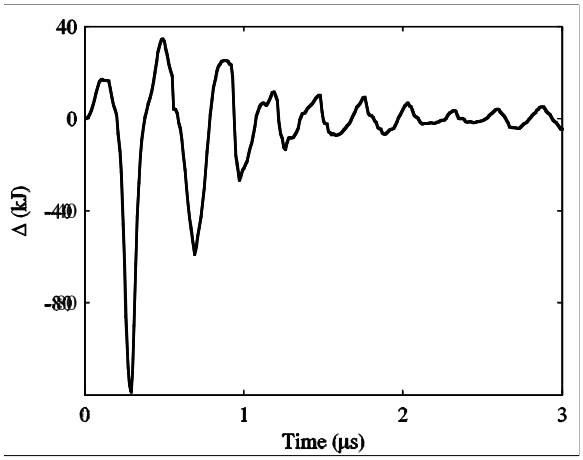

Fig. 5. The quantity delta vs. time, which approaches zero as equilibrium is established.

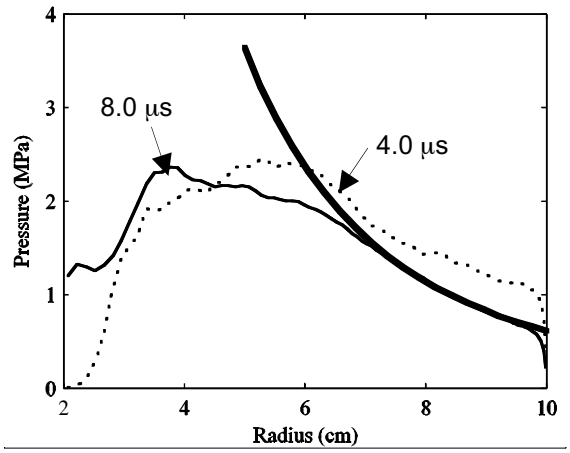

Fig. 6. Graphs of z-averaged pressure vs. radius at different times. By 8 microseconds the plasma has settled into a stable profile that closely matches the Kadomtsev Q=1 marginal state at large radius (indicated with heavy line). At smaller radius the value of Q is less than 1.

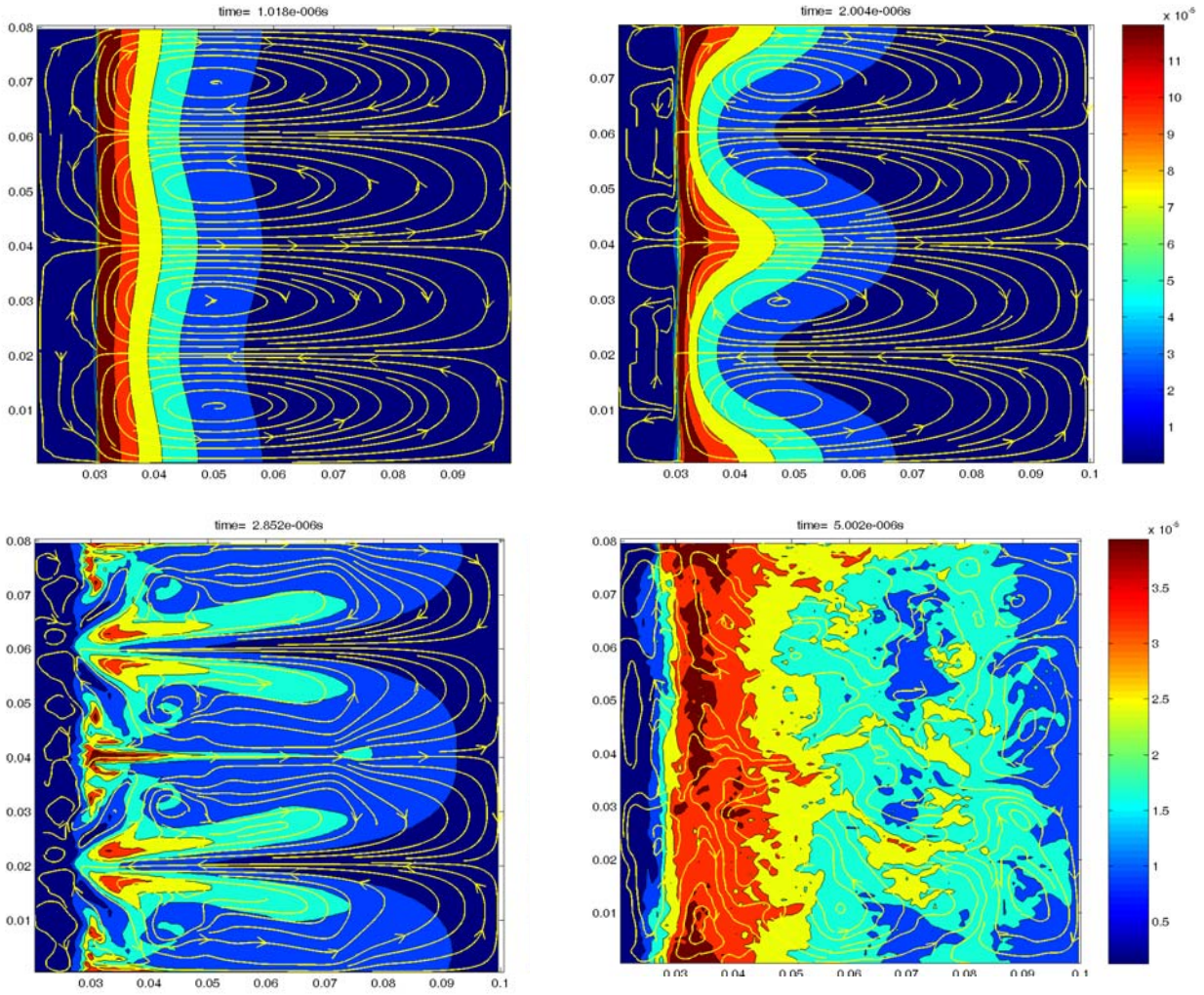


Fig. 7. Contour plots in r and z of density (color) combined velocity stream lines showing interchange motion of instability for the idealized initial conditions.